2013 European Control Conference (ECC)
July 17-19, 2013, Zürich, Switzerland.

Reference Governor Design for Computationally Efficient Attitude and Tether Tension Constraint Enforcement on a Lighter-Than-Air Wind Energy System

(Invited Paper)

Uroš Kalabić Chris Vermillion Ilya Kolmanovsky

***Abstract*— In this paper, we propose a reference governor-based approach to guarantee enforcement of critical flight constraints on the Altaeros tethered, lighter-than-air wind energy system. While the high-altitude flight made available by the tethered system leads to significant increases in power production over traditional, tower-mounted systems, the freedom of motion resulting from the tethers and aerodynamic shell introduces critical attitude and tether tension constraints. To date, methods considered for enforcing these constraints have relied upon heuristic static maps or model predictive control (MPC). The former cannot guarantee transient constraint satisfaction, whereas the latter is computationally burdensome given Altaeros's current microcontroller capabilities. The approach pursued in this paper uses a reference governor, which is a computationally simple add-on to the existing controller that enforces transient and steady-state constraints. The methodology proposed in this paper is demonstrated through simulations on linear and nonlinear models of the longitudinal dynamics of the Altaeros system with wind gust disturbances.**

I. Introduction

Wind represents a substantial source of new renewable energy installations, accounting for a record 42 percent of new U.S. energy installations and 26 percent of new E.U. energy installations in 2012. Still, limitations on ground-level wind speeds and large tower installation costs have motivated the study of tethered, high-altitude airborne wind energy systems, described in [1]-[11]. Based on studies presented in [12] and [13], wind at 600m altitude carries upwards of 5 times the power density of ground level wind in many locations. Furthermore, tethered systems offer the advantage of rapid deployability, which makes them an attractive alternative to diesel generators for off-grid and short-term applications, including oil and gas exploration, military bases, and disaster relief.

This paper considers the Altaeros system, shown in Fig. 1, which uses a buoyant shroud to elevate a horizontal axis turbine to altitudes up to 600m. The full Altaeros system consists of a rotating base station which houses winches that regulate the release of tethers leading to the shroud.

Although Altaeros's Helium shroud provides constant buoyancy approximately equal to 120 percent of the shroud's weight (under normal atmospheric conditions), it is essential in high wind speeds that the system maintains non-negative aerodynamic lift through an acceptable angle of attack. Furthermore, it is important that the tethers remain in an acceptable tension range where they neither become slack, resulting in a loss of controllability, nor exceed structural limitations.

Fig. 1. Photograph of Altaeros's proof-of-concept system, which was flown at Loring Air Force Base during the winter of 2012.

Several control strategies have been proposed in an effort to track setpoints while satisfying the aforementioned constraints. In [10], a heuristically-designed hierarchical control system is proposed, wherein a static outer loop controller maps setpoints to a steady-state flying envelope, and an inner loop controller performs setpoint tracking. This strategy

This research was supported by the National Science Foundation, Award Number 1130160.

U. Kalabić and I. Kolmanovsky are with the Department of Aerospace Engineering, University of Michigan, Ann Arbor, MI 48109, USA. Email: {ilya,kalabic}@umich.edu

C. Vermillion is with Altaeros Energies, Boston, MA 02210, USA. Email: chris.vermillion@altaerosenergies.com

was successfully flight-tested in winter, 2012; however, the proposed control strategy provided no guarantee of constraint satisfaction. In order to provide guaranteed transient constraint enforcement, a model predictive control (MPC) strategy is proposed in [11], which does indeed guarantee transient constraint satisfaction but also is computationally burdensome.

This paper presents a reference governor approach for guaranteeing transient constraint satisfaction with simple compuations. The approach adjusts altitude and pitch angle setpoints in order to satisfy pointwise-in-time state and control input constraints, including constraints on altitude, angle of attack and tether tensions. The reference governor serves as an add-on to a closed-form base controller, which is designed using LQ techniques in this paper. Under realistic bounds on the wind speed disturbance, the approach guarantees that these important system constraints are satisfied during both transient and steady-state operations. Ultimately, this reference governor-based approach accomplishes constraint enforcement under a fraction of the computational load that is required by the MPC algorithm of [11]. In this paper, we apply the reference governor to the longitudinal system dynamics, which dominate the motion of the system once it has been stabilized to a downwind condition (see [10] for a discussion of techniques for attacking the important problem of stabilization to a downwind condition).

The paper is organized as follows. Section II provides a general mathematical description for the reference governor approach, which will be subsequently tailored specifically to the model and constraints of the Altaeros system. Section III provides the details of the longitudinal dynamic model, and Section IV describes the control design, which leverages the linearized dynamic model along with the mathematical ingredients from Section II. Section V provides simulation results on the linearized model, and Section VI provides the results of simulations on the nonlinear model. These results demonstrate that the reference governor does an effective job of ensuring that critical state constraints are enforced.

II. Reference Governors

Reference governors (RGs) [14], [15] (for a more complete list of references on this topic, see [16]) are add-on predictive control schemes that enforce pointwise-in-time constraints based on discrete-time linear models of the form,

$$x(t+1) = Ax(t) + Bv(t) + B_w\bar{w}(t), \quad (1)$$

$$y(t) = Cx(t) + Dv(t) + D_w\bar{w}(t) \in Y, \ \forall t \in \mathbb{Z}_+, \quad (2)$$

where $x(t) \in \mathbb{R}^n$ is the system state, $v(t) \in \mathbb{R}^m$ is the reference set-point, and $\bar{w}(t) \in W$ is a set-bounded disturbance where W is some compact set satisfying $0 \in W$. The upper-bar notation on $\bar{w}(t)$ is used to distinguish the disturbance from the vertical body-fixed velocity, which is denoted by w. The set $Y \subset \mathbb{R}^p$ denotes a compact and convex set of output constraints and $\mathbb{Z}_+ = \{0, 1, 2, \dots\}$ is the set of non-negative integers. The transition matrices are all appropriately sized and C and D are chosen so that $y(t)$ is a vector of all variables that are to be constrained; in this way, the RG handles coupled state-control constraints.

Fig. 2 shows RG placement with respect to the closed-loop system. Given a state estimate or measurement, $\hat{x}(t)$, the RG modifies a desired set point, $r(t)$, to obtain the constraint-admissible set-point $v(t)$. In this paper, the closed-loop system block represents the coupled dynamics of the plant and LQ controller.

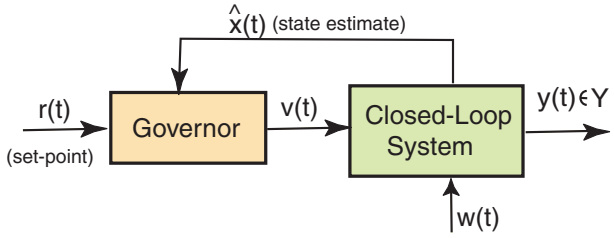

Fig. 2. Schematic of RG placement with respect to a closed-loop system

At each time-step, the RG computes a constraint-admissible $v(t)$ for a given desired set-point, $r(t)$. It does this through the use of the maximal constraint-admissible set,

$$O^a_\infty = \{(x(0), v) : v(t) \equiv v, \quad (1)\text{-}(2) \text{ are satisfied, } \forall\{\bar{w}(t)\} \in \mathcal{W}\}, \quad (3)$$

where $\mathcal{W} = \{\bar{w}(t) \in W : t \in \mathbb{Z}_+\}$ is the set of all possible future disturbance sequences.

O^a_∞ is the set of all initial state and constant reference pairs for which the constraint $y(t) \in Y$ is satisfied for all present and future time. The idea of the RG is, given a current state measurement or estimate, $x(t)$, to find the reference satisfying $v(t) \in \Pi(x(t))$ where,

$$\Pi(x) = \{v : (x, v) \in O^a_\infty\}. \quad (4)$$

The offline computation of O^a_∞ is basedon,

$$O^a_\infty = O_{t^*}, \quad (5)$$

where O_{t^*} is calculated through the following recursive algorithm,

$$O_{t+1} = O_t \cap Y_{t+1}, \qquad O_0 = Y_0, \quad (6)$$

$$Y_{t+1} = Y_t \sim CA^tB_wW, \qquad Y_0 = Y \sim D_wW, \quad (7)$$

where $\sim$ denotes the Pontryagin (or Minkowski) difference[1]. From the definition of the P-difference and (7), we can see that the computation of O^a_∞ and $\Pi(x)$ assumes the worst-case disturbance, so that the RG is robust to any possible disturbance sequence. This is a somewhat conservative assumption and in Section V, we consider a relaxed design of the RG. The finite determination time, t^*, is the minimum time t for which O_t satisfies the definition in (8); for purposes of the algorithm, t^* is the first time for which $O_t = O_{t+1}$, *i.e.* $t^* = \inf\{t \in \mathbb{Z}_+ : O_{t+1} = O_t\}$. To guarantee finite

[1]The P-difference of two sets, $U, V \in \mathbb{R}^n$, is: $U \sim V = \{z : z + v \in U, \ \forall v \in V\}$

t^*, a slightly tightened constraint on $v(t)$ may need to be augmented (see [17]).

If Y is polyhedral, then O^a_∞ and $\Pi(x)$ are also polyhedral [17], [15], [18] and can be characterized by a finite set of linear inequalities,

$$O^a_\infty = \{(x, v) : H_x x + H_r v \leq h\}, \tag{8}$$
$$\Pi(x) = \{v : H_r v \leq h - H_x x\}. \tag{9}$$

In this case the algorithm for computing O^a_∞ reduces to the offline solution of a finite number of linear programming problems [17], [18].

The computation of O^a_∞ is performed offline. Online, the RG updates $v(t)$ according to,

$$v(t) = v(t-1) + \kappa(t)(r(t) - v(t-1)), \tag{10}$$

where the RG algorithm performs the optimization,

$$\max \kappa(t) \in [0, 1] \text{ subject to } v(t) \in \Pi(x(t)). \tag{11}$$

If the previous constraint-admissible value, $v(t-1)$, has been initialized correctly, then the optimization is explicitly solveable [14], [15] and is the solution of a finite number of scalar division problems. The reference $v(t-1)$ is initialized either at the initial time $t = 0$ before the RG begins operation or calculated by the RG during the previous time step.

Lastly, the RG guarantees finite-time convergence to a constant reference: If the desired reference is constant, $r(t) \equiv r$, then $v(t)$ monotonicaly converges to r in finitely many time-steps.

III. Longitudinal Dynamic Model

The longitudinal dynamic model used in this paper is based on the model introduced in [10] and is briefly discussed in this section. The model components and variables are summarized in Table I. Because this paper focuses on the treatment of the system longitudinal dynamics, the model of [10] is reduced to the 10 states that are relevant when the dynamic behavior is restricted to the vertical x-z plane. Furthermore, this work on the longitudinal system assumes synchronized port and starboard tether motions, and therefore the control space is limited to 2 control variables. The subscript i (used with control inputs, tether tensions, and unstretched lengths) denotes a particular tether set, where $i = 1$ represents the forward tether set and $i = 2$ represents the aft tether set.

Nonlinear Shroud Dynamics

The shroud dynamics follow a standard 3-degree-of-freedom model in which the body-fixed x and z axes are in the direction of the aft and top of the shroud, respectively. The rotational equations of motion are given by:

$$\dot{\theta} = q, \tag{12a}$$
$$\dot{q} = \frac{1}{I_{yy}}(M^{aero}_y + M^{tether}_y + M^b_y), \tag{12b}$$

TABLE I
Key Model Variables

Component	Variable	Description
Shroud	x_g,z_g	ground-fixed c.m. pos.
States	u,w	body-fixed c.m. velocity
	θ	pitch angle
	q	pitch rate
Winch	l_i	tether i unstretched length
States	$\bar{v}_i$	tether i release speed
Tether	T_i	tether i tension
Control	$\bar{u}_i$	winch speed command
Disturbances	u_{wind}	horizontal wind speed
	w_{wind}	vertical wind speed

where I_{yy} represents the moment of inertia and M^{aero}_y, M^{tether}_y, and M^b_y respectively represent the total aerodynamic, tether-generated, and buoyancy-generated moments about the y-axis.

The translational equations of motion are given by,

$$\dot{u} = -wq + \frac{1}{m}(F^{eb}_x + F^{aero}_x + F^{tether}_x), \tag{13a}$$
$$\dot{w} = uq + \frac{1}{m}(F^{eb}_z + F^{aero}_z + F^{tether}_z), \tag{13b}$$

where m represents the shroud mass and $F^{eb}_{x,z}$, $F^{aero}_{x,z}$, and $F^{tether}_{x,z}$ respectively represent the excess buoyant (buoyant force minus gravitational force), aerodynamic, and tether forces along both axes. Using the rotation matrix associated with θ, the body-fixed velocities are easily converted to ground-fixed coordinates, and x_g and z_g are readily calculated through integration.

Winch and Tether Spooling Dynamics

The winches comprise AC motors that drive a drum and regulate the unstretched line length of each of the control tethers. They are governed by the following equations.

$$\dot{l}_i = \bar{v}_i, \tag{14a}$$
$$\dot{\bar{v}}_i = \frac{1}{\tau_{winches}}(\bar{u}_i - \bar{v}_i). \tag{14b}$$

Here, $\tau_{winches}$ represents the approximate actuator time constant associated with the winches, which is taken as 0.1 seconds for this work.

Tether Tension Calculation

The tethers are modeled, as in [19], [20], as spring-dampers that can assume only positive tension. Specifically, the tether tension is given by:

$$T_i = \max\big(0,\ k_{tethers}(\|\mathbf{r}^{shroud}_i - \mathbf{r}^{bs}_i\| - l^{unstretched}_i) + b_{tethers}\frac{d}{dt}\|\mathbf{r}^{shroud}_i - \mathbf{r}^{bs}_i\|\big), \tag{15}$$

where $\mathbf{r}^{shroud,bs}_i$ represents the ground-fixed 2-dimensional coordinate vector of the shroud and base station tether attachment points for tether i, $k_{tethers}$ represents the tether stiffness, and $b_{tethers}$ represents the tether damping. Stiffness

TABLE II

NOMINAL OPERATING POINT FOR LINEARIZED MODEL

System parameters	Nominal values
$u_{wind,0}$	20
$w_{wind,0}$ (m/s)	0
$l_{i,0}^{unstretched}$ (m)	595
$x_{g,0}$ (m)	258
$z_{g,0}$ (m)	543
α_0 (°)	10.8
$T_{1,0}$ (N)	10852
$T_{2,0}$ (N)	8113
$\bar{u}_{i,0}$ (m/s)	0

and damping terms are taken to be equal for the forward and aft tethers.

Linearized System Dynamics

The reference governor design for the Altaeros system is based on linear models. In this paper, we consider the linearizations of the longitudinal dynamics of the system about a representative operating condition summarized in Table II.

The continuous-time linear model of the system has the following form,

$$\dot{x}(t) = A_c x(t) + B_c \bar{u}(t) + B_{c,w} \bar{w}(t), \tag{16}$$

$$y(t) = Cx(t) + D\bar{u}(t) + D_w \bar{w}(t). \tag{17}$$

The components of the output vector $y(t)$ are the variables to be constrained. These are deviations in the altitude ($\delta z_g(t)$), Front Tether Tension ($\delta T_1(t)$), Aft Tether Tension ($\delta T_2(t)$), angle of attack ($\delta\alpha(t)$), Front Tether Rate ($\delta\bar{u}_1(t)$), and Aft Tether Rate ($\delta\bar{u}_2(t)$) from the nominal conditions. The components of the input vector $\bar{u}(t)$ for the linear model are the commanded Front Tether Rate ($\bar{u}_1(t)$) and the Aft Tether Rate ($\bar{u}_2(t)$). As with the disturbance, $\bar{w}(t)$, the upper bar notation is used in $\bar{u}(t)$ in order to distinguish the control input vector from the body-fixed x velocity, denoted by u. The 10 states in (16) are denoted by $x(t)$. The components of the disturbance vector $\bar{w}(t)$ are the deviations of the Base Wind speed ($\delta u_{wind}(t)$) and the Vertical Wind speed ($\delta w_{wind}(t)$) from the nominal wind speeds, about which the linearization was taken.

In the simulations, the wind speed disturbances are modeled using a Dryden turbulence model, summarized in [21], which characterizes the spectral properties of turbulence as a function of altitude and base wind speed. This is incorporated into the model by passing band-limited white noise through coloring filters whose parameters are directly related to turbulence intensity, scale length, and base wind speed. Fig. 3 shows the wind speed disturbance inputs.

System Constraints

A summary of the system constraints follows. The altitude is constrained to a limit of 609m, arising from an FAA limit of 2000ft above ground level for moored balloons. The angle of attack is constrained to between 0° and 20°, where the limits correspond to insufficient lift and stall, respectively.

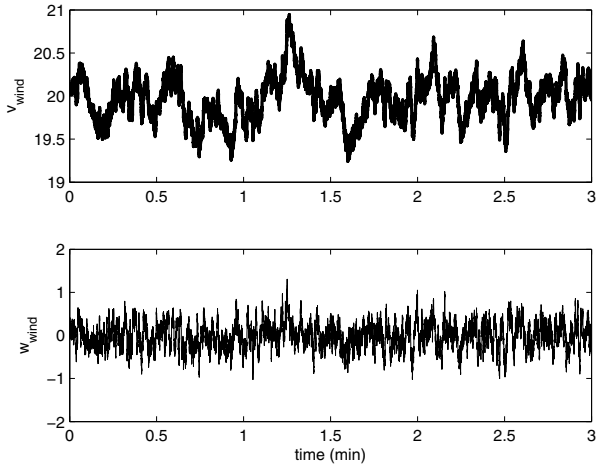

Fig. 3. Horizontal (top) and vertical (bottom) wind speeds

The tether tensions, T_i, are constrained to between 100N and 20kN, where the lower limit prevents slack tethers, with a margin for robustness, and the upper limit arises from material limitations. Finally, the control inputs, $\bar{u}_i$, are constrained to between $\pm$1m/s, in order to account for saturation limits.

The constraint set Y from (2) is given as, $Y = \{y(t) : 0 \leq z_{g,0} + \delta z_g \leq 609,\ 0 \leq \alpha_0 + \delta\alpha \leq 20,\ 100 \leq T_{i,0} + \delta T_i \leq 20000,\ -1 \leq \bar{u}_{i,0} + \delta\bar{u}_{i,0} \leq 1,\ i = 1, 2\}$. Note that Y is polyhedral.

IV. CONTROLLER DESIGN

Baseline Controller Design

To begin the controller design, the system (16)-(17) is discretized using a zero-order hold using a sampling time of $T_s = 0.1$s.

The base controller is designed, using LQ techniques, to track set-points for altitude and pitch commands. Define the constraint-admissible and reference command, respectively as,

$$v(t) = \begin{bmatrix} \delta z_{g,gov}(t) \\ \delta\theta_{gov}(t) \end{bmatrix},\ r(t) = \begin{bmatrix} \delta z_{g,d}(t) \\ \delta\theta_d(t) \end{bmatrix}. \tag{18}$$

Let C_r be such that $C_r x(t) = (\delta z_g(t), \delta\theta(t))$. Since $\bar{u}(t)$ are rate inputs, we design the tracking controller so that $C_r x(t) \to r(t)$ while $\bar{u}(t) \to 0$. This proceeds by defining error dynamics, $e(t+1) = e(t) + C_r x(t) - r(t)$, and coupling them with (16) to obtain,

$$\begin{bmatrix} e(t+1) \\ x(t+1) \end{bmatrix} = \begin{bmatrix} I & C_r \\ 0 & A \end{bmatrix} \begin{bmatrix} e(t) \\ x(t) \end{bmatrix} + \begin{bmatrix} 0 \\ B \end{bmatrix} \bar{u}(t) - \begin{bmatrix} I \\ 0 \end{bmatrix} r(t). \tag{19}$$

The nominal controller is a linear quadratic regulator to minimize,

$$J = \frac{1}{2} \sum_{t=0}^{\infty} \left(e^{\mathrm{T}}(t) Q_e e(t) + x^{\mathrm{T}}(t) Q x(t) + \bar{u}^{\mathrm{T}}(t) R \bar{u}(t) \right) dt, \tag{20}$$

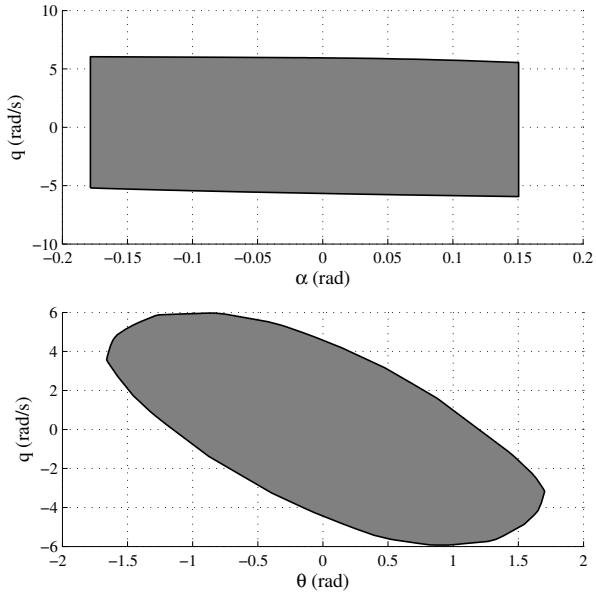

Fig. 4. Projections of O_∞^a onto the α-q (top) and θ-q (bottom) planes.

for $r(t) \equiv 0$, where $Q_\varepsilon, Q \succeq 0$ and $R \succ 0$, so that the control is of the following form,

$$\bar{u}(t) = -K_e e(t) - Kx(t). \tag{21}$$

Note that this controller achieves zero tracking error for constant commands $r(t)$, due to the fact that the plant contains an integrator.

V. Linear Model Simulation

The following results correspond to a 3 minute simulation with reference inputs, $r(t)$, given in Fig. 5 and disturbances, $\bar{w}(t)$, given in Fig. 3. Practical considerations have governed the selection of the disturbance set as $W = [-0.2, 0.2]^2$ and two projections of the resulting O_∞^a corresponding to the linear system are provided in Fig. 4. To avoid conservatism in the RG response and recognizing that wind velocity does not change instantaneously between extreme values as assumed in the theory of the RG, the choice of W is set to the rms of the expected disturbance (corresponding to one standard deviation), which is approximately 0.13. The size of W has been slightly increased in order to ensure that it provides adequate protection against simulated wind disturbances. Future work will focus on incorporating a more elaborate disturbance model in a RG design that will enforce constraints less conservatively.

The results are given in Figs. 5-9. Fig. 5 shows the constraint-admissible reference, $v(t)$, as calculated by the RG.

Overall, this set of simulations demonstrates that the RG keeps the system responses within acceptable bounds over the course of setpoint changes superimposed on top of realistic wind disturbance scenarios. On the other hand, the ungoverned system exhibits every variety of constraint violation at some point. Fig. 6 shows improved tracking and

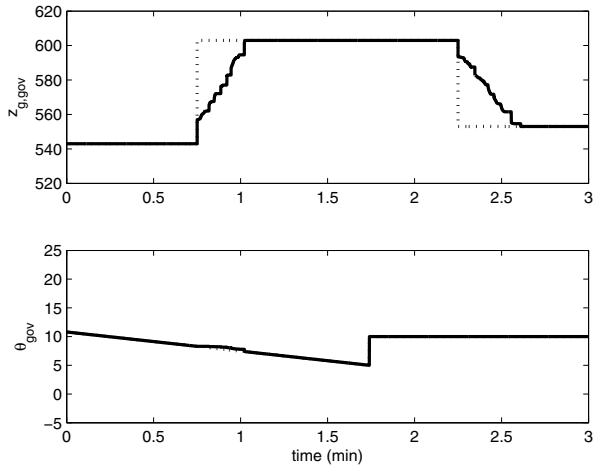

Fig. 5. Desired (dotted) and governed (solid) reference inputs for $z_{g,d}(t)$ (top) and $\theta_d(t)$ (bottom)

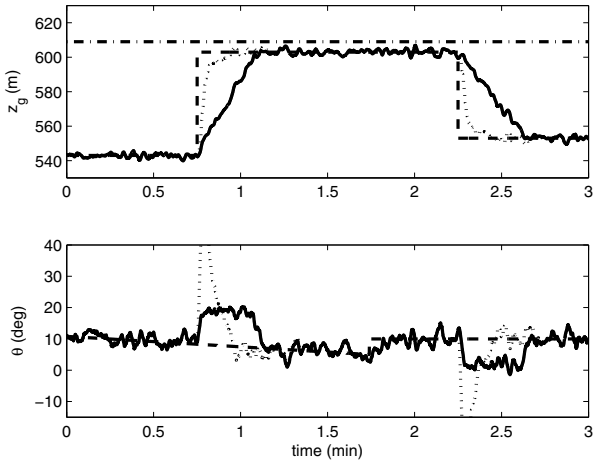

Fig. 6. z_g and θ ungoverned (dotted) and governed (solid) response plotted against desired set-point $r(t)$ (dashed) and the altitude constraint (dot-dashed)

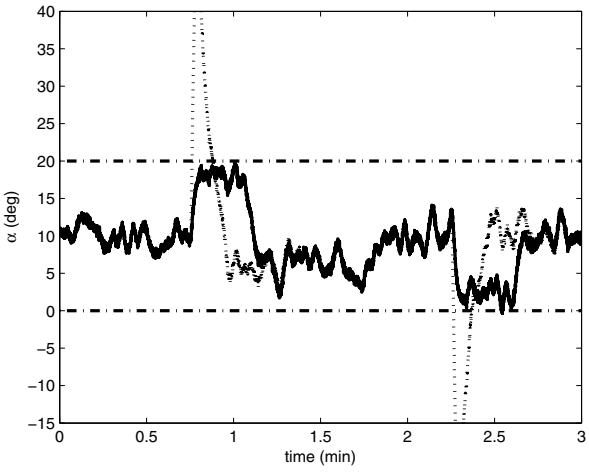

Fig. 7. $\alpha(t)$ ungoverned (dotted) and governed (solid) response plotted against constraints (dot-dashed)

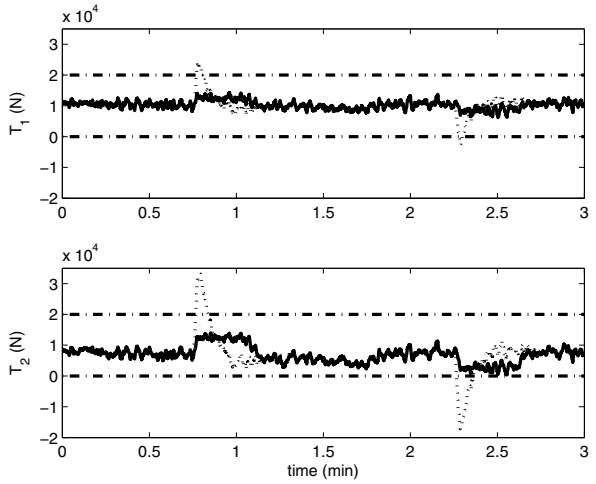

Fig. 8. Forward (top) and Aft (bottom) tension ungoverned (dotted) and governed (solid) responses plotted against constraints (dot-dashed). Note that the magnitudes of negative tether tensions do not carry physical significance but rather merely reflect the fact that the tethers are slack; these negative values arise due to the use of the linearized model.

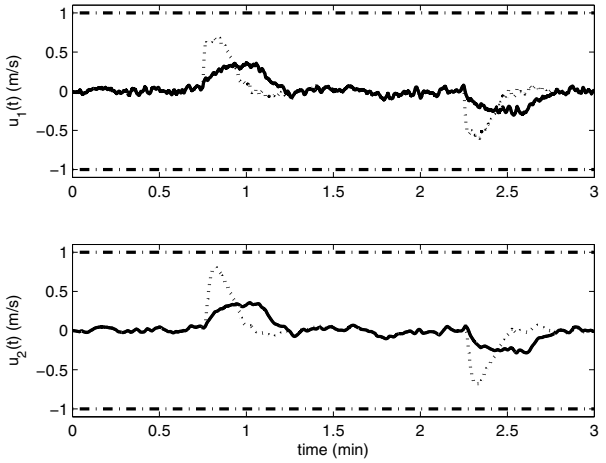

Fig. 9. $\bar{u}_1(t)$ (top) and $\bar{u}_2(t)$ (bottom) ungoverned (dotted) and governed (solid) responses plotted against saturation limits (dot-dashed)

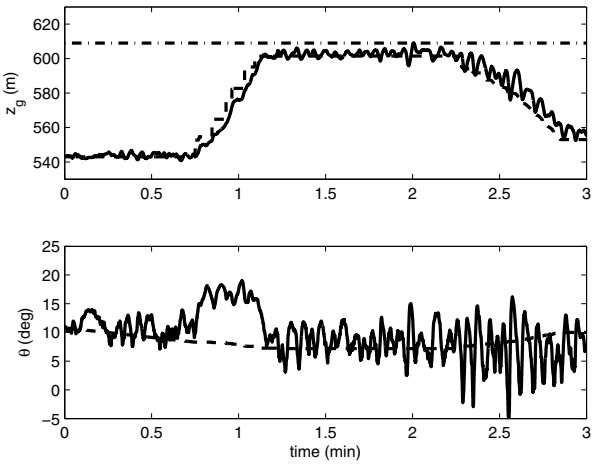

Fig. 10. z_g and θ response (solid) plotted against governed set-point $r(t)$ (dashed) and the altitude constraint (dot-dashed)

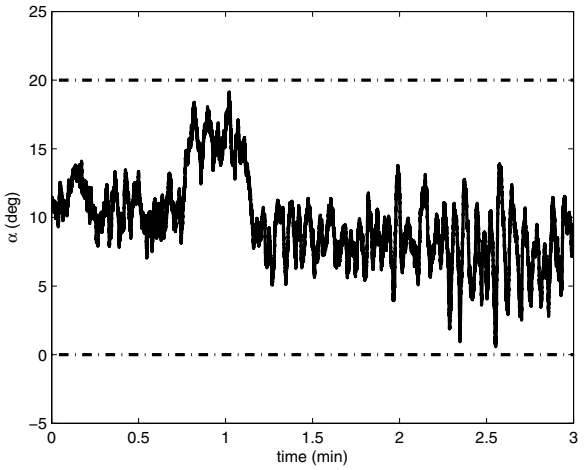

Fig. 11. $\alpha(t)$ response plotted against constraints (dot-dashed)

constraint satisfaction with the RG, whereas the ungoverned controller exhibits transient altitudes that exceed the FAA limitation of 2000ft AGL. Furthermore, Fig. 7 shows that while the ungoverned controller exhibits severe angle of attack ($\alpha(t)$) violations upon altitude setpoint changes, the RG keeps $\alpha(t)$ within acceptable bounds in order to prevent the loss of lift that results from stall or a nose-down configuration. Finally, Fig. 8 demonstrates that both tether tensions remain within acceptable bounds upon altitude changes, whereas the ungoverned response exhibits slack tethers and excessive tether tensions at different times. It is important to note that although the linearized model generates negative tension, the magnitude of these negative values do not carry physical significance; they merely reflect slack tethers.

VI. Nonlinear Model Simulation

Although extensions of RG theory to nonlinear systems exist [22], in this section we present a simpler and less computationally expensive method, in which a linear RG with a few modifications is used to predict constraint violation. Firstly, we develop a Kalman filter to estimate the output $y(t)$ and use the nonlinear model output as an input to the oberver. The RG is consequently applied to the observer estimate. We also tighten the constraint on $\alpha(t)$ to the set $[3, 17]$ instead of $[0, 20]$ and lower the altitude constraint to 604m, because closer to constraints, these two variables are more sensitive to inputs than they are at the operating point.

Furthermore, we do not present ungoverned response results because the application of the above controller without an RG results in nonrobust operation; specifically, its application leads the system to stall, which ultimately causes catastrophic loss of lift. The results are presented in Figs. 10-13.

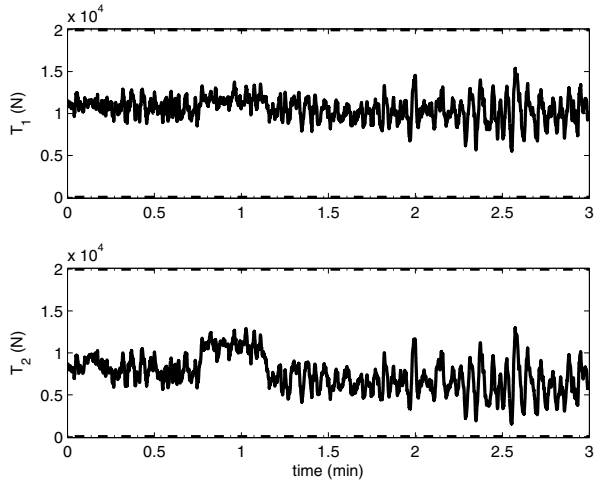

Fig. 12. Forward (top) and Aft (bottom) tension responses plotted against constraints (dot-dashed)

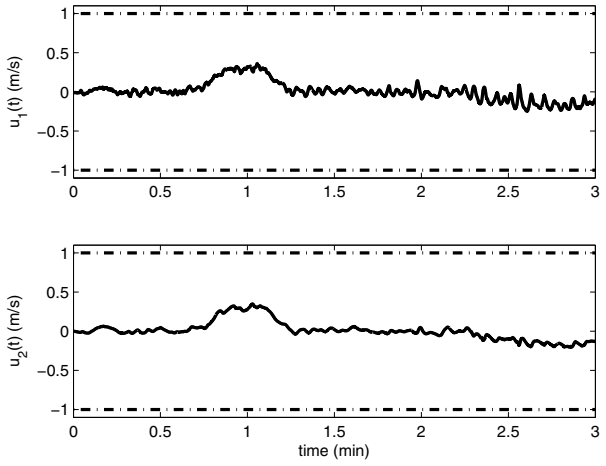

Fig. 13. $\bar{u}_1(t)$ (top) and $\bar{u}_2(t)$ (bottom) responses plotted against saturation limits (dot-dashed)

The results show similar response properties to that found in Section V, demonstrating that all state and control input constraints are successfully enforced by the RG. The success of the approach on the fully nonlinear model indicates promise for the practical application of the RG approach in future flight testing.

VII. Conclusions and Future Work

This paper has presented a reference governor (RG)-based approach for guaranteeing that critical flight constraints are satisfied by the Altaeros system. The RG is a computationally simple scheme that is added to nominal control design in order to enforce constraint adherence. The paper detailed the RG design formulation and demonstrated the satisfaction of critical altitude, tether tension, and angle of attack constraints in the presence of realistic setpoint variations and wind disturbance inputs in the context of a longitudinal dynamic model. Future work will include the validation of the proposed strategy on the full 6 degree-of-freedom nonlinear model and a comprehensive comparison between the computationally simple heuristic and RG approaches and the more computationally intensive model predictive control (MPC) strategies, including those in our earlier work [11].

References

[1] P. Williams, B. Lansdorp, and W. Ockels, "Modeling and control of a kite on a variable length flexible inelastic tether," *AIAA Modeling and Simulation Technologies Conf. and Exhibit*, Hilton Head, SC, 2007, AIAA-2007-6705.

[2] P. Williams, B. Lansdorp, and W. Ockels, "Optimal cross-wind towing and power generation with tethered kites," *J. Guid. Control Dynam.*, vol. 31, no. 1, pp. 81–93, 2008.

[3] M. Canale, L. Fagiano, M. Milanese, and M. Ippolito, "KiteGen project: Control as key technology for a quantum leap in wind energy generators," in *Proc. American Control Conf.*, New York, NY, 2007, pp. 3522–3528.

[4] M. Canale, L. Fagiano, and M. Milanese, "High altitude wind energy generation using controlled power kites," *IEEE Trans. Control Syst. Technol.*, vol. 18, no. 2, pp. 279–293, 2010.

[5] L. Fagiano, "Control of tethered airfoils for high-altitude wind energy generation," Ph.D. dissertation, Dept. Control and Comp. Eng., Poly. U. Turin, Italy, 2009.

[6] A. Ilzhofer, B. Houska, and M. Diehl, "Nonlinear MPC of kites under varying wind conditions for a new class of large-scale wind power generators," *Int. J. Robust Nonlin.*, vol. 17, no. 17, pp. 1590–1599, 2007.

[7] S. Gros, M. Zanon, and M. Diehl, "Orbit Control for a Power Generating Airfoil Based on Nonlinear MPC," in *Proc. American Control Conf.*, Montreal, QC, 2012, pp. 137–142.

[8] S. Brabeck, "SkySails – Ship propulsion by automated towing kites," Presented at 2012 Airborne Wind Energy Conf., Leuven, Belgium.

[9] C. Hardham, "Advances in crosswind power generation," Presented at 2012 Airborne Wind Energy Conf., Leuven, Belgium.

[10] C. Vermillion, T. Grunnagle, and I. Kolmanovsky, "Modeling and control design of a lighter-than-air wind energy system," in *Proc. American Control Conf.*, Montreal, QC, 2012, pp. 5813–5818.

[11] R. Weng. K. Balasubramanian, C. Vermillion, and I. Kolmanovsky, "Model predictive longitudinal control of a lighter-than-air wind energy system," in *Proc. ASME Dynamic Syst. and Control Conf.*, Fort Lauderdale, FL, 2012.

[12] C. L. Archer and K. Caldeira, "Atlas of high altitude wind power," Carnegie Institute for Science, Stanford, CA, 2008.

[13] C. L. Archer and K. Caldeira, "Global Assessment of High-Altitude Wind Power," *Energies*, vol. 2, no. 2, pp. 307–319, 2009.

[14] E. G. Gilbert, I. V. Kolmanovsky, and K. T. Tan, "Discrete-time reference governors and the nonlinear control of systems with state and control constraints," *Int. J. Robust Nonlin.*, vol. 5, no. 5, pp. 487–504, 1995.

[15] E. G. Gilbert and I. V. Kolmanovsky. "Fast reference governors for systems with state and control constraints and disturbance inputs," *Int. J. Robust Nonlin.*, vol. 9, no. 15, pp. 1117–1141, 1999.

[16] I. Kolmanovsky, U. Kalabić, and E. Gilbert, "Developments in constrained control using reference governors," in *Proc. IFAC Conf. Nonlinear Model Predictive Control*, Noordwijkerhout, Netherlands, 2012, pp. 282–290.

[17] I. Kolmanovsky and E. G. Gilbert, "Theory and computation of disturbance invariant set of discrete-time linear systems," *Math. Probl. Eng.*, vol. 4, no. 7, pp. 317–367, 1998.

[18] E. G. Gilbert and C. J. Ong. "Linear systems with hard constraints and variable set points: Their robustly invariant sets," Dept. of Mech. Eng., Nat. Univ. Singapore, Tech. Rep. C08-002, 2008.

[19] P. Dewdney, M. Nahon, and B. Veidt, "The large adaptive reflector: A giant radio telescope with an aero twist," *Can. Aeronaut. Space J.*, vol. 48, no. 4, pp. 239–250, 2002.

[20] M. Nahon, G. Gilardi, and C. Lambert, "Dynamics/control of a radio telescope receiver supported by a tethered aerostat," *J. Guid. Control Dynam.*, vol. 25, no. 6, pp. 1107–1115, 2002.

[21] "Flying qualities of piloted airplanes," U.S. Military Spec. MIL-F-8785C, 1980.

[22] E. G. Gilbert and I. V. Kolmanovsky, "Nonlinear tracking control in the presence of state and control constraints: a generalized reference governor," vol. 38, no. 12, pp. 2063–2073, 2002.